Polarization field effects at liquid-crystal-droplet–polymer interfaces

Mourad Boussoualem,[1] Mimoun Ismaili,[2] Jean-François Lamonier,[3] Jean-Marc Buisine,[2] and Frédérick Roussel[1,*]
[1]*Laboratoire de Thermophysique de la Matière Condensée, UMR CNRS 8024, MREI, Université du Littoral-Côte d'Opale, 59140 Dunkerque, France*
[2]*Laboratoire de Dynamique et Structure des Matériaux Moléculaires, UMR CNRS 8024, Bât P5, Université de Lille 1, 59655 Villeneuve d'Ascq, France*
[3]*Laboratoire de Catalyse et Environnement, E.A. 2598, MREI, Université du Littoral-Côte d'Opale, 59140 Dunkerque, France*
(Received 15 October 2004; published 3 April 2006)

The influence of confinement (droplet size) and liquid crystal orientational order (smectic-*A* and nematic) on the interfacial polarization field effects [Maxwell-Wagner-Sillars (MWS) effect] existing in liquid-crystal-droplets–polymer systems is investigated by broadband dielectric spectroscopy and a forward transmittance measurement technique. A relaxation process observed in the low frequency domain of the dielectric spectrum has been associated with a MWS effect for both micron-size and submicron-size droplets. Using electro-optical measurements and numerical simulations of the field inside droplets, it is shown that a depolarization field takes place in the same frequency range as that determined by dielectric spectroscopy. Differential scanning calorimetry measurements allowed to estimate the phase-separated liquid crystal [4,4′-octylcyanobiphenyl (8CB)] fraction, which was found in the range of 55% for both micron-size and submicron-size droplets. X-ray diffraction experiments showed that smectic 8CB confined to micron-size cavities adopt bulklike properties, i.e., a partial bilayer structure, whereas in submicron-size droplets the layer spacing of the smectic phase is increased due to the strong bending deformations induced by the high curvature of the cavity walls.

DOI: 10.1103/PhysRevE.73.041702 PACS number(s): 61.30.Pq, 64.70.Md, 77.22.−d, 78.20.Jq

I. INTRODUCTION

Interfacial polarization field effects, also known as the Maxwell-Wagner-Sillars (MWS) effect, are commonly observed in heterogeneous systems due to the accumulation of charges at the interfaces between phases giving rise to polarization [1,2]. This phenomenon is of main scientific interest from both fundamental and applied point of views because it plays a crucial role on the electrical or electro-optical properties of numerous materials such as semiconducting glasses [3], semicrystalline polymers [4], biological cell suspensions [5], or liquid crystal (LC) dispersions [polymer-dispersed liquid crystals (PDLC), holographic PDLC, or arrays of polymer-encapsulated liquid crystals] [6–10]. In their most common form, LC dispersion films consist of low molecular weight liquid crystal dispersed as micrometer (or nanometer)-sized droplets within a polymer matrix. Electro-optical (EO) devices based on these systems basically work by switching between scattering and transparent states upon application of a sufficiently large electric field which reorient the director field in the droplets index matching the droplets and polymer matrix. These composite materials have found great interest because of their promising use in advanced optical device applications such as large flexible displays or paperlike displays for electronic books.

Among the main aspects governing the EO properties of LC dispersion films are the droplet size and shape, the boundary conditions at the polymer-LC interface, and the dielectric characteristics of the composite in alternating electric fields [11–13]. For sufficiently small droplets, thermodynamic phases can be induced or suppressed by the confinement, and Golemme *et al.* [14] provided experimental demonstration that the isotropic-nematic transition is even replaced by a continuous evolvement of order for submicron-size LC drops. Liquid crystal molecules in contact with a solid substrate often adopt a preferred direction of alignment which depends on subtle molecular interactions between the LC and the host. Three types of alignment have been observed, i.e., the molecular main axis is oriented either normal to the interface (homeotropic anchoring), or parallel to the interface (planar or homogeneous anchoring) or along a tilted direction. In the case of LC dispersions, LC molecules are first anchored at the polymer interface and second confined to a curved geometry which leads to topological defects in the director-field configuration. The cavity surface is then a strong determining factor that is closely related to the order parameter of the confined LC phase [12]. Finally, the switching of LC droplets requires application across the film of an electric field, E, capable of overcoming the elastic forces of LC leading to a configuration of lower free energy and then to a reorientation of the director. However, it has been demonstrated theoretically and experimentally that the field inside a LC droplet is strongly frequency dependent [13,15]. For example, LC and polymer conductivity effects, giving rise to polarization at the droplet interface, are invariably suppressed at high enough frequencies whereas they can dominate the dielectric terms at low frequencies and low resistivities. This phenomenon strongly affects the EO performances of LC dispersions and can even be detrimental to technological developments for some polymer-LC formulations because most of these devices are usually driven by 50–100 Hz electric fields (i.e., close to domestic household ac voltage frequencies).

*Electronic address: frederick.roussel@univ-littoral.fr

In this paper, the morphology and the physical properties of a polymer/LC model system have been studied by polarized optical microscopy (POM), differential scanning calorimetry (DSC), and x-ray diffraction (XRD) experiments. The influence of confinement (droplet size) and LC orientational order (smectic-*A* or nematic) on the interfacial polarization field effects is investigated by broadband dielectric spectroscopy and a forward transmittance measurement technique. Based on a self consistent field approximation, numerical simulations of the field inside droplets are performed and correlated to dielectric and electro-optical data.

II. EXPERIMENT

The single component liquid crystal chosen for this work is 4-*n*-octyl-4′cyanobiphenyl (8CB) (Frinton Laboratories, NJ) because it exhibits both nematic and smectic orders. Polystyrene (PS) was used as polymer matrix because it presents several advantages compared to other thermoplastic compounds such as low dc and ac conductivities ($\sigma_{dc} \approx 10^{-18}$ S cm^{-1}; $\sigma_{ac} \approx 10^{-9}$ S cm^{-1}), a dielectric permittivity remaining unchanged ($\epsilon \sim 2.5$) in both temperature (24–80 °C) and frequency (1 kHz–100 MHz) ranges of interest, and commercially available well-characterized monodisperse samples ($M_w = 200\,000$ g mol^{-1}, $I_p = 1.05$; Aldrich). PS and 8CB in a given weight percent ratio were dissolved in a common solvent [tetrahydrofuran (THF)] at 50 wt % then stirred mechanically for 12 h prior to solvent evaporation for 24 h. The dried mixture in the isotropic state was introduced by capillarity into calibrated 50 μm thick transparent conducting (ITO) commercial cells (EHC, Japan) at 70 °C. After complete filling of the cell, the sample was cooled from the isotropic state to 0 °C at a rate of either −2 °C min^{-1} to produce micron-size droplets or −80 °C s^{-1} to get submicron-size droplets. The droplet size and the phase transitions of the PS/8CB mixtures were studied by polarized optical microscopy (Leica DMRXP microscope equipped with a heating or cooling stage Linkam LTS-350) and differential scanning calorimetry (DSC Q1000, TA Instruments). The structure of the confined liquid cristalline phases were determined by XRD experiments performed at $T = 25$ °C on a Bruker D8 Advance diffractometer [Cu Kα1 radiation (1.5405 Å)]. The scattering intensities were recorded on the angular range $0.8 \leqslant 2\theta \leqslant 60°$ with a step-size of $\Delta(2\theta) = 0.01°$ and a count time of 6 s per step. The real (ϵ') and imaginary (ϵ'') parts of the complex dielectric permittivity $[\epsilon^*(\omega) = \epsilon'(\omega) - j\epsilon''(\omega)]$ of PS/8CB mixtures were recorded with a HP 4192A impedance or gain-phase analyzer generating a 100 mV sinusoidal voltage in the frequency range 5 Hz→13 MHz. Temperature control of the capacitor was achieved with a Mettler Toledo FP82HT/FP90 setup. The Havriliak-Negami analysis was applied for the quantitative interpretation of the dielectric data to determine the corresponding mean relaxation rates (f_c) and dielectric strengths $[\Delta\epsilon = (\epsilon_s - \epsilon_\infty)]$ of the relaxation processes. The EO properties of PS/8CB films were determined from time-resolved, forward transmittance of a He-Ne laser beam passing through the film, while applying across the film a sinusoidal voltage modulated in amplitude by a triangular wave ($V_{\mathrm{rms}} = 140$ V, 1.67×10^{-2} Hz).

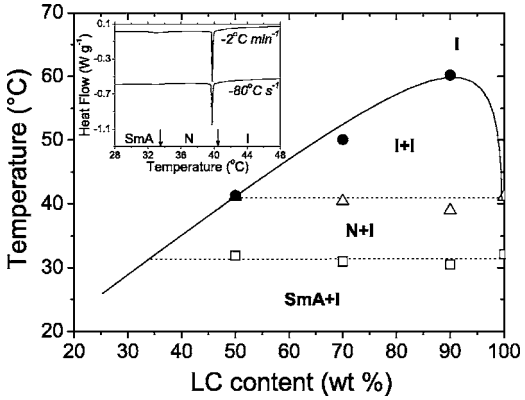

FIG. 1. Phase diagram of PS-8CB obtained from POM observations. Symbols are averages of two series of samples from separate experiments. Solid and dotted lines are guides to the eyes. The phase diagram exhibits four distinct domains: Smectic-*A* +isotropic (Sm*A*+*I*), nematic+isotropic (*N*+*I*), isotropic +isotropic (*I*+*I*), and isotropic (*I*), where Sm*A*, *N*, and *I* refer to the phase separated LC domains, and *I* is associated with the homogeneous polymer rich phase. Inset: DSC thermograms of a PS-8CB (30:70) sample cooled either at a rate of −2 °C min^{-1} (micron-size droplets) or −80 °C s^{-1} (submicron-size droplets). Vertical arrows indicate the phase transition temperatures of pure 8CB provided by the manufacturer.

III. RESULTS AND DISCUSSION

A. Phase diagram and morphology

Figure 1 displays the equilibrium phase diagram of PS-8CB mixtures in the form of temperature versus LC weight fraction. The symbols represent averages of POM and DSC data (heating/cooling rates set at 2 °C min^{-1}), whereas solid and dotted lines are guides to the eyes. The diagram exhibits an upper critical solution temperature (UCST) with four distinct regions: Smectic-*A*+Isotropic (Sm*A*+*I*, 21.5 °C →32.5 °C), nematic+isotropic (*N*+*I*, 32.5 °C→39.5 °C), isotropic+isotropic (*I*+*I*, 39.5 °C→63 °C), and isotropic (*I*, above 63 °C). As displayed in Fig. 2 (top), POM observations have shown that the LC droplet size of a PS-8CB (30:70) mixture cooled at a rate of −2 °C min^{-1} is in the micrometer range. When the same mixture is quenched from the isotropic state to 0 °C at a rate of −80 °C s^{-1}, the texture of the sample [Fig. 2 (bottom)] observed between crossed polarizers appears mostly black, i.e., mostly isotropic, with tiny isolated birefringent spots. In order to get further insight on the phase separation process leading to this texture, DSC measurements have been carried out to estimate the phase-separated LC fractions [16]. For comparison, typical thermograms of a PS-8CB (30:70) mixture cooled at a rate of either −2 °C min^{-1} or −80 °C s^{-1} are displayed in the inset of Fig. 1. Both systems display transformations which can be assigned to the polymer-dispersed 8CB, evidencing that a phase-separation mechanism occured. From the enthalpy change measurements performed on the first orderlike tran-

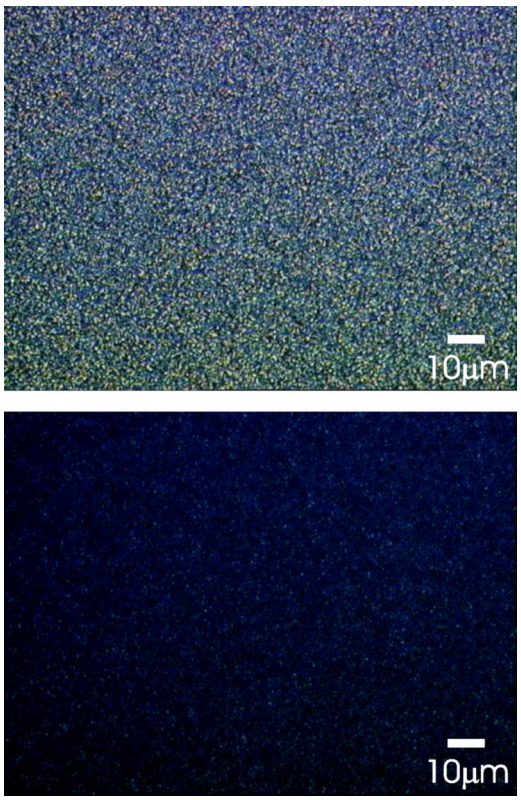

FIG. 2. (Color online) Optical micrographs of a PS-8CB (30:70) sample cooled at a rate of either $-2\ ^{\circ}\mathrm{C\ min^{-1}}$ (top) or $-80\ ^{\circ}\mathrm{C\ s^{-1}}$ (bottom) [crossed polarizers mode ($P \perp A$), magnification $\times 320$, $T=25\ ^{\circ}\mathrm{C}$ (Sm$A+I$ domain)].

sition detected at $T \approx 39\ ^{\circ}\mathrm{C}$ (mesogenic to isotropic state transformation), the LC fraction contained in the droplets was calculated. Average values were found in the range of $55\% \pm 2\%$ for both systems which is in good agreement with values reported in the literature for similar PS/LC mixtures [13,17]. Considering DSC results and POM observations, it can be reasonnably assumed that the liquid crystal dispersions obtained from PS-8CB mixtures cooled at a rate of $-80\ ^{\circ}\mathrm{C\ s^{-1}}$ exhibit a morphology where the LC droplet size is close to, or smaller than the optical resolution of the microscope, i.e., in the submicrometer range.

It is known that the confinement induced in very small droplets strongly affects the physical properties of the phase-separated liquid crystal compound [14]. In particular, the structure of the confined LC phase can be drastically modified in highly curved geometries. Due to its orientational and positional order, the smectic-A phase is expected to experience important structural changes in submicron-size drops. In order to investigate the structural characteristics of confined 8CB, x-ray diffraction experiments were performed on a PS-8CB (30:70) mixture cooled at a rate of either $-2\ ^{\circ}\mathrm{C\ min^{-1}}$ or $-80\ ^{\circ}\mathrm{C\ s^{-1}}$. Figure 3 shows typical XRD patterns recorded at $T=25\ ^{\circ}\mathrm{C}$, i.e., in the Sm$A+I$ region (see Fig. 1). In the case of micron-size droplets (top pattern), a sharp reflection (a) is first observed at low angle. A periodicity of $d=30.5$ Å was measured, i.e., ≈ 1.4 times the fully extended molecular length of 22.1 Å. This result shows that confined 8CB molecules adopt a partial bilayer structure in

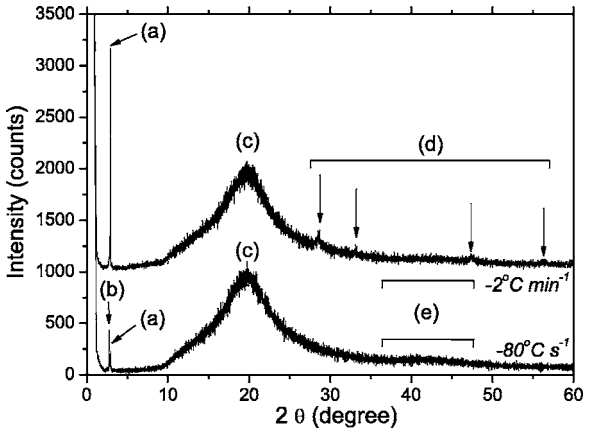

FIG. 3. X-ray diffraction patterns recorded at $T=25\ ^{\circ}\mathrm{C}$ of a PS-8CB (30:70) sample cooled at a rate of either $-2\ ^{\circ}\mathrm{C\ min^{-1}}$ (top) or $-80\ ^{\circ}\mathrm{C\ s^{-1}}$ (bottom).

the smectic-A phase as reported in the literature for pure 8CB [18].

Therefore, it can be reasonnably concluded that the sharp reflection (a) observed in the small angle region of the XRD pattern corresponds to the stacking period of the smectic layers in the SmA phase. The presence of a broad diffusion band (c) at about 5 Å ($2\theta \approx 20°$) seems to indicate that 8CB molecules mostly adopt a liquid like ordering within the smectic layers [19]. However, in the high angle region many small reflections (d) are also observed. These signals are an indication of a partial two-dimensional ordering of the molecules within the smectic layers. A deeper analysis is then necessary to ascertain the exact nature of these reflections. Further XRD experiments are currently in progress to decipher this problem. In addition, it is worth noting the presence of a very diffuse scattering band (e) which can be related to the existence of π-π interactions between phenyl rings of 8CB molecules [19].

In the case of submicron-size droplets (Fig. 3, bottom), the pattern is modified compared to that of micron-size cavities, indicating that the SmA ordering is strongly perturbated by the confinement. In particular, the intensity of reflection (a) is ten times smaller, and a sharp reflection (b) is observed at a lower angle and with a higher intensity ($\times 2$) than (a). A smectogenic structure with a layer spacing of $d=32.1$ Å is then formed as well as a smectic-A ordering which is very limited in its growth. This behavior can be explained by the high curvature of submicron-size droplets which induces strong bending deformations of the smectic layers. The SmA layers are likely formed within a small region near the cavity center, whereas the smectogenic structure obviously takes place near the cavity walls.

B. Dielectric properties

Figure 4 displays the evolution of the dielectric strength $\Delta\epsilon$ versus temperature corresponding to the relaxation process observed in the low frequency region of the dielectric spectrum (inset of Fig. 4) of PS/8CB films cooled at a rate of either $-2\ ^{\circ}\mathrm{C\ min^{-1}}$ (micron-size droplets) or $-80\ ^{\circ}\mathrm{C\ s^{-1}}$

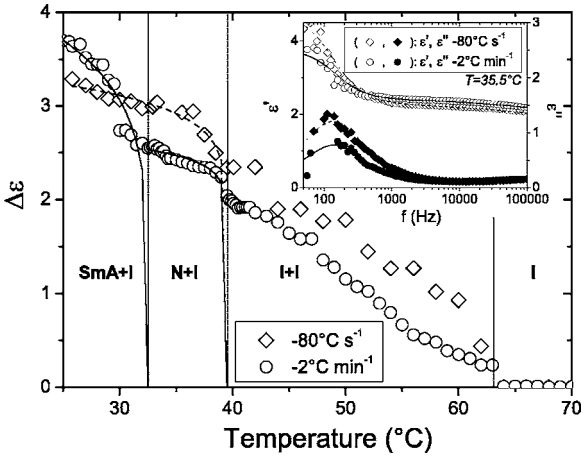

FIG. 4. Temperature dependence of the dielectric strengths $\Delta\epsilon$ of the relaxation process observed in the low frequency region for a 50 μm thick [PS/8CB (30:70)] film cooled at a rate of -2 °C min^{-1} (○; micron-size droplets) and -80 °C s^{-1} (◇; submicron-size droplets), respectively. The solid and dashed lines are Haller-type fit curves (see text). The vertical dotted lines represent the phase transition temperatures as observed by optical microscopy. Inset: Real (ϵ') and imaginary (ϵ'') parts of the complex permittivity of the same PDLC film in the frequency range 50 Hz→100 kHz at T =35.5 °C. Open (ϵ') and filled (ϵ'') symbols are experimental data whereas the solid and dashed lines are Havriliak-Negami fit curves.

(submicron-size droplets). For both systems, a low frequency relaxation process is observed (see inset of Fig. 4) indicating that this phenomenon exists for any droplet size. Recalling that PS/8CB mixtures exhibit a heterogeneous morphology consisting of LC droplets dispersed in a continuous polymer-rich phase, accumulation of charges at the interfaces between phases obviously occurs giving rise to polarization which contributes to relaxation. This phenomenon, also known as the Maxwell-Wagner-Sillars effect [1,2], originates from restricted motion of charge carriers at interface boundaries. Due to its slow relaxation process, this mechanism is observed in the low frequency region of the dielectric spectrum. In order to confirm this assignment, increasing bias voltages were applied leading to a decrease in the dielectric strength $\Delta\epsilon$. According to previous results [13], this behavior can be explained by the fact that dipoles associated with the electrical charges located at the droplet interfaces are further aligned along the bias field with increasing bias voltage. This result confirms that the low frequency relaxation mechanism is associated with charges (conductivity effects) and corresponds to a MWS effect. In the region where LC phases are observed and considering the evolution of the experimental data, the temperature dependence of the dielectric strength $\Delta\epsilon$ was fitted to a Haller-type equation [12,20]

$$\Delta\epsilon \propto S \approx S_0(1-(T/T_{tr}))^F, \tag{1}$$

where $S_0(\propto\Delta\epsilon_0)$ is the limit of the order parameter with decreasing temperature, T_{tr} is the transition temperature, and F may be considered as an indication of how quickly charges reach the limit of the order parameter of the confined phase as a function of change in temperature. A good agreement was found in both SmA+I and N+I region between the experimental data and the solid and dashed lines (Fig. 4) which are the best fit curves using a Haller-type equation. According to these results, it clearly appears that the MWS polarization field is closely related to the order parameter of the confined LC phase. Another interesting feature is that the evolution of $\Delta\epsilon$ with temperature depends on the LC droplet size. In the case of micron-size droplets (○, solid line), the SmA-N transition is clearly observed whereas in the case of submicron-size droplets (◇, dashed line) a continuous evolvement of $\Delta\epsilon$ vs T is obtained instead of an abrupt transition. For submicron-size droplets, the $\Delta\epsilon_0$ (3.522) and F (0.086) values (see Table I) retrieved from the data fits were found between those determined for micron-size SmA and N domains indicating that an intermediate order between the SmA and N structures takes place. This observation is in good agreement with XRD experiments, which show that a smectogenic order mostly takes place in submicron-size cavities. Also, it has been reported in the literature [21] that LC molecules in contact with a PS surface usually adopt a planar anchoring which means that in submicron-size droplet a smectogenic structure would be favored. Therefore, confinement effects play a crucial role on the order parameter of the segregated LC phase and as a consequence on the polarization fields existing at the polymer-LC interfaces. Interestingly, the amplitude of the dielectric strength associated with the polarization field increases when the LC phase exhibits a higher order parameter (nematic, smectogenic, smectic-A). Recalling that the electrical conductivity is a key point for the charge accumulation process at the droplet interfaces, and taking into account that the SmA phase is observed at a lower temperature than the N phase, these results seem to

TABLE I. Parameters for the temperature dependence of $\Delta\epsilon$ obtained from fitting the experimental data (see Fig. 4) to Haller-type equation. Experimentally, the limiting value of $\Delta\epsilon_0$ cannot be reached due to phase transition into a lower temperature phase. The factor F describes how fast the order parameter and then $\Delta\epsilon$ of the polarization field changes with temperature. E_A is the activation energy retrieved from the relaxation rate data (see Fig. 5).

	Submicron-size droplets			Micron-size droplets		
Phase	$\Delta\epsilon_0$	F	E_A (kJ mol^{-1})	$\Delta\epsilon_0$	F	E_A (kJ mol^{-1})
SmA+I	3.522	0.086	24.5	4.775	0.173	13
N+I	3.522	0.086	24.5	2.774	0.054	37
I+I			20			30

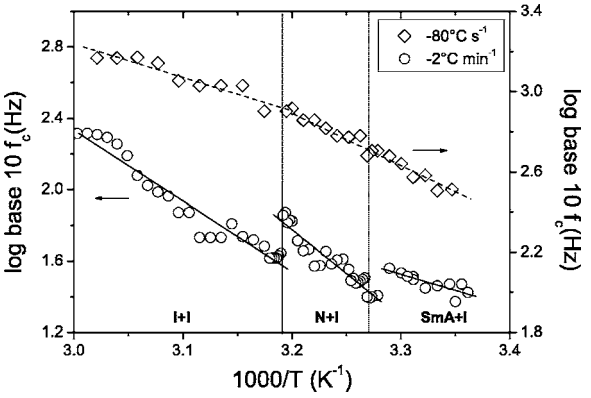

FIG. 5. Arrhenius plot of the temperature dependence of the MWS relaxation frequency f_c of a 50 μm thick [PS/8CB (30:70)] film cooled at a rate of $-2\ ^\circ\mathrm{C\ min^{-1}}$ (○, left axis; micron-size droplets) or $-80\ ^\circ\mathrm{C\ s^{-1}}$ (◇, right axis; submicron-size droplets), respectively.

indicate that the confinement of mesophases exhibiting a higher order parameter (e.g., Sm*A*) enhances interfacial polarization effects.

In the $I+I$ region, $\Delta\epsilon$ follows a linear decrease with increasing temperature for both droplet sizes until to become null when the sample reaches the I state. The linear decrease of $\Delta\epsilon$ can be explained by the diminution of the density number of isotropic LC droplets with increasing temperature due to an improved miscibility between the LC and the polymer at high temperature [13]. Above $T=63\ ^\circ$C (I region), the sample is fully homogeneous (see Fig. 1) meaning that interfacial polarization-field effects do not exist, and then $\Delta\epsilon=0$. This result clearly shows the close relationship between the dropletlike morphology and the relaxation mechanism observed at $\approx$200 Hz associated with a polarization process resulting from a charge accumulation at the polymer/droplet interface. The temperature dependence of the relaxation frequency f_c (Fig. 5) is another factor indicating that a MWS effect occurs. Indeed, the evolution of $\log_{10}(f_c)$ vs $1/T$ exhibits Arrhenius-like behaviors for both micron-size and submicron-size droplets. According to activation energies E_A retrieved from the relaxation frequency data fits (Table I), the relaxation process asssociated with the polarization field (MWS effect) is enhanced for micron-size droplets in the smectic phase compared to that in the N phase ($E_A^{\mathrm{Sm}A+I} \ll E_A^{N+I}$). This means that the charge motion is favored in the Sm*A* phase increasing the polarization field effects at polymer/droplet interfaces. For the submicron-size droplets, a single activation energy value was found ranging between those of Sm$A+I$ and $N+I$ domains. This result is consistent with DSC and XRD measurements confirming that strongly confined 8CB molecules preferably adopt a smectogenic order which evolves continuously in the LC region.

In the case of micron-size droplets, one has discontinuities of the relaxation rate at the phase transition temperatures. Similar discontinuities have been reported in the literature for bulk LC phases and explained by the difference of viscosity between the Sm*A*, *N*, and *I* phases, respectively [22,23]. In contrast, these discontinuities are smeared out for the submicron-size cavities, showing the drastic influence of the confinement on the LC viscosity characteristics. This behavior can be explained by the strong elastic forces existing in restricted geometries whereas bulklike properties are observed in micron-size droplets. Then, the measurement of the relaxation rate allows to evidence the viscosity changes at phase transitions which strongly affect the charge motion and then polarization-field effects at the polymer/LC interface.

C. Electro-optics

In order to investigate the influence of polarization-field effects on the EO behavior of PS/8CB mixtures, transmittance versus applied voltage measurements have been carried out on films exhibiting either a smectic-*A* or a nematic phase. In the case of micron-size droplets, LC molecules inside the droplets (Sm*A* and *N*) reorient upon application of an external sinusoidal field (1 kHz) leading to a typical sigmoidal curve shape plot for the transmittance versus E [6]. In the case of submicron-size droplets, the transmittance remains constant even upon application of high field ($E > 6\ \mathrm{V\ \mu m^{-1}}$). The director reorientation process does not take place because of the strong elastic forces existing in submicron-size cavities which can not be overcome by the applied electric field. Using the self consistent field approximation, the field inside a spherical micron-size droplet E_i can be estimated for a sinusoidal applied field [1,24]

$$E_i(\omega) = \frac{3\epsilon_M^*}{\epsilon_{LC}^* + 2\epsilon_M^* - \phi_{LC}(\epsilon_{LC}^* - \epsilon_M^*)} E_a \exp(-j\omega t), \quad (2)$$

where ϕ_{LC} is the phase separated LC fraction ($\phi_{LC}\sim 0.55$), E_a is the magnitude of the applied field ($E_a=V_a/d$), and $\epsilon_M^* = \epsilon_M' - j\frac{\sigma_M'}{\omega\epsilon_0}$, and $\epsilon_{LC}^* = \epsilon_\parallel' - j\frac{\sigma_\parallel'}{\omega\epsilon_0}$, where ϵ_M' and $\epsilon_\parallel'$ are the dielectric permittivities of the PS matrix and LC aligned along E_a, respectively, and σ_M' and $\sigma_\parallel'$ are the electrical conductivities of the PS matrix and LC aligned along E_a, respectively. Using micron-size droplet films, the sinusoidal voltage applied across the film was set so that the film exhibits a maximum tansmittance (T_{max}), then the frequency was varied from 1 kHz to 1 Hz. As shown in Fig. 6, T_{max} decreases with decreasing frequency. The frequency range to switch the film from a transparent to a scattering state varies from 100 $\rightarrow$20 Hz for N droplets and from 70$\rightarrow$2 Hz for Sm*A* droplets. This behavior can be explained by the presence of charges located at the polymer/LC interfaces (MWS effect) which will move under the influence of the external field (conductivity effect), setting up a depolarization field across the film. At high frequencies, conductivity effects become unimportant relative to dielectric effects because the charge motion is frozen out. In comparison, conductivity effects dominate the dielectric terms at low frequency leading to a depolarization field which will tend to cancel the applied field. In both Sm*A* and *N* domains, a good agreement is found between experimental transmittance data and E_i/E_a simulated curves confirming that the low frequency relaxation process is closely related to a depolarization field. The frequency downshift of $\sim$50 Hz observed between the EO reponses of Sm*A* and *N* micron-size droplets is a consequence of a higher conductivity of the Sm*A* phase compared

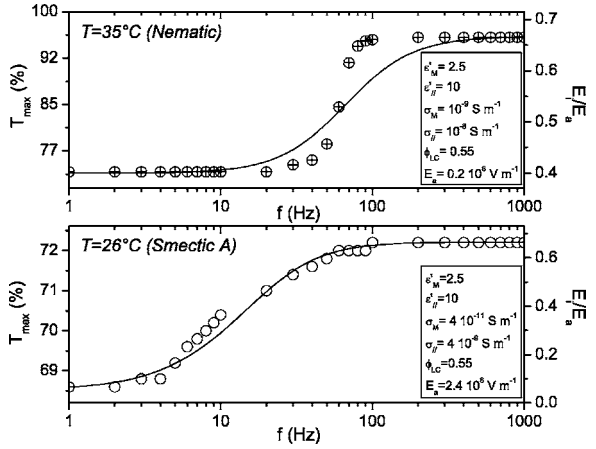

FIG. 6. Frequency dependence of the maximum transmittance T_{max} (symbols, left axis) and the simulated field [Eq. (2)] inside a spherical droplet (E_i) over sinusoidal applied field (E_a) (lines, right axis) of a 50 μm thick [PS/8CB (30:70)] exhibiting micron-size droplets at $T=26$ °C [Sm*A* phase (bottom)] and $T=35$ °C [*N* phase (top)].

to that of the *N* phase. This leads to an enhanced relaxation process (lower E_A) and then to an increased depolarization field. The strong frequency dependence of the EO properties drastically influences the operation of PS/8CB devices showing the ability to drive LC dispersions films by applying sinusoidal voltages of suitable frequencies.

IV. CONCLUSION

In summary, POM, DSC, and XRD experiments have been carried out on a polymer/LC model system to investigate the morphology and the physical properties of the phase-separated LC phase. Depending on the cooling rate used (-2 °C min^{-1} or -80 °C s^{-1}) to prepare the PS/8CB sample, the phase separation mechanism involved leads to a droplet-like morphology with micron-size or submicron-size domains, respectively. For both temperature treatments, the phase-separated LC fraction of a PS/8CB (30:70) mixture was found in the range of 55%. The structural characteristics of confined 8CB have been investigated by XRD experiments at $T=25$ °C, i.e., in the smectic phase. In the case of micron-size droplets, 8CB molecules adopt bulklike properties, i.e., a partial bilayer structure, whereas for the submicron-size droplets the layer spacing of the smectic phase increases due to the strong bending deformations induced by the high curvature of the cavity walls. The dielectric properties of PS/8CB films exhibiting micron-size or submicron-size droplets have been studied by ac impedance spectroscopy. The presence of a low frequency relaxation process has been attributed to interfacial polarization-field effects originating from restricted motion of charge carriers at polymer/LC interface boundaries. The temperature dependence of the dielectric strength $\Delta\epsilon$ of this relaxation process has shown the close relationship between the droplet-like morphology and the existence of a MWS relaxation mechanism. Another interesting feature is the dependence of $\Delta\epsilon$ with the order parameter of the confined LC phase and LC droplet size. First, the confinement of mesophases exhibiting a higher order parameter enhances interfacial polarization effects, and, second, a smectogenic order mostly takes place in submicron-size cavities as evidenced by XRD experiments. Relaxation rate measurements have demonstrated that the charge motion is favored in the Sm*A* phase, as well as the confinement strongly influences the LC viscosity properties. In particular, the viscosity change at phase transitions affects the charge motion and then polarization-field effects at the polymer/LC interface. The influence of the MWS effect on the electro-optical behavior of PS/8CB mixtures has been investigated using maximum transmittance versus frequency measurements and compared to numerical simulations of the electric field inside spherical droplets. A good agreement has been found between experimental data and simulated curves showing that the motion of charges located at polymer/LC interfaces under the influence of the applied external field sets up a depolarization field across the entire film. This depolarization field has been unambiguously assigned to the low frequency relaxation process (MWS effect) observed in the dielectric spectrum. The agreement of dielectric data, EO response and numerical simulation offers interesting insights on the interfacial polarization field-effects, enlightening the role of the confinement and the order parameter of the segregated phase in heterogeneous systems such as anisotropic droplets–polymer dispersions.

ACKNOWLEDGMENTS

The authors acknowledge the Ministère de la Recherche, the Communauté Urbaine de Dunkerque, the EU program Interreg III, and the CNRS for financial support.

[1] B. K. P. Scaife, *Principles of Dielectrics* (Clarendon Press, Oxford, 1989).
[2] F. Kremer and A. Schönhals, *Broadband Dielectric Spectroscopy* (Springer-Verlag, Berlin, 2003).
[3] M. Sayer and A. Mansingh, Phys. Rev. B **6**, 4629 (1972).
[4] E. Neagu, P. Pissis, L. Apekis, and J. L. Gomez Ribelles, J. Phys. D **30**, 1551 (1997).
[5] K. Asami, in *Handbook on Ultrasonic and Dielectric Characterization Techniques for Suspended Particules*, edited by V. A. Hackley and J. Texter (The American Ceramic Society, Westerville, OH, 1999), p. 333.
[6] P. S. Drzaic, *Liquid Crystal Dispersions* (World Scientific, Singapore, 1995).
[7] O. Levy, Phys. Rev. Lett. **86**, 2822 (2001).
[8] C. C. Bowley and G. P. Crawford, Appl. Phys. Lett. **76**, 2235 (2000).
[9] A. Fernández-Nieves, D. R. Link, D. Rudhardt, and D. A. Weitz, Phys. Rev. Lett. **92**, 105503 (2004).

[10] D. Rudhardt, A. Fernández-Nieves, D. R. Link, and D. A. Weitz, Appl. Phys. Lett. **82**, 2610 (2003).
[11] K. Amundson and M. Srinivasarao Phys. Rev. E **58**, R1211 (1998).
[12] F. Roussel, C. Canlet, and B. M. Fung, Phys. Rev. E **65**, 021701 (2002); F. Roussel and B. M. Fung, *ibid.* **67**, 041709 (2003).
[13] M. Boussoualem, F. Roussel, and M. Ismaili, Phys. Rev. E **69**, 031702 (2004).
[14] A. Golemme, S. Žumer, D. W. Allender, and J. W. Doane, Phys. Rev. Lett. **61**, 2937 (1988).
[15] O. Levy, Phys. Rev. E **61**, 5385 (2000); Eur. Phys. J. E **3**, 11 (2000).
[16] F. Roussel, J. M. Buisine, U. Maschke, X. Coqueret, and F. Benmouna, Phys. Rev. E **62**, 2310 (2000).
[17] F. Benmouna *et al.*, Macromolecules **33**, 960 (2000).
[18] P. J. Collings, *Liquid Crystals* (IOP Publishing Ltd, Bristol, 1990).
[19] L. Larios-López *et al.*, Liq. Cryst. **30**, 423 (2003).
[20] T. Bräuniger and B. M. Fung, J. Chem. Phys. **102**, 7714 (1995).
[21] M. Oh-e, S.-C. Hong, and Y. R. Shen, Appl. Phys. Lett. **80**, 784 (2002).
[22] J. Jadżyn, L. Hellemans, G. Czechowski, C. Legrand, and R. Douali, Liq. Cryst. **27**, 613 (2000).
[23] J. Jadżyn and G. Czechowski, Phys. Rev. E **64**, 052702 (2001).
[24] J. Kelly and D. Seekola, Proc. SPIE **1257**, 17 (1990).